Journal of ELECTRONIC MATERIALS, Vol. 48, No. 9, 2019
https://doi.org/10.1007/s11664-019-07405-1

Formation and Evolution of Cu-Sn Intermetallic Compounds in Ultrasonic-Assisted Soldering

WEIYUAN YU,[1,2] YINGZONG LIU,[1] and YUN LIU[1]

1.—State Key Laboratory of Gansu Province, Advanced Processing and Recycling of Nonferrous Metals, Lanzhou University of Technology, Lanzhou 730050, Gansu Province, People's Republic of China. 2.—e-mail: weiyuanyu2018@163.com

Interfacial intermetallic compounds (IMCs) help determine the reliability of soldered joints; thus, it is necessary to understand their formation and evolution. This study focus on Cu-Sn IMCs formed in ultrasonic-assisted soldering (UAS), wherein the formation of IMCs at the Sn/Cu interface is controlled by changing the ultrasonic action time. After being subjected to ultrasonic vibration, the IMCs at the Cu/Sn solid–liquid interface are continuously crushed, dissolved, and formed, which occurs successively in the Cu_6Sn_5 and Cu_3Sn layers. The relationship between the thickness of the IMC layer and ultrasonic action time in Cu-Sn samples was identified. Simultaneously, the growth pattern of Cu_6Sn_5 grains in the Sn solder is transformed, and the tin solder (Sn solder) is kept in a dynamic non-equilibrium state with IMCs at the Sn/Cu interface through UAS. More Cu_6Sn_5 grains formed and were evenly distributed in the joint after cooling, which improves the performance of the joints.

Key words: Ultrasonic-assisted soldering, interfacial intermetallic compounds, microstructure, tin solder

INTRODUCTION

The reliability and thermal fatigue lifetime of solder joints has a major effect on the service life of electronic devices; the interfacial intermetallic compound (IMC) layer of the joints has an especially significant effect on the reliability of soldered joints.[1,2] The Cu/Sn/Cu system of electronic packaging has been systematically studied in recent decades, showing that Sn solder reacts with the Cu substrate to generate Cu-Sn IMCs, including Cu_6Sn_5 and Cu_3Sn.[3–5] Excessively thick IMC layers seriously reduce the reliability of soldered joints, or a thinner IMC layer is difficult to ensure connection reliability between the Cu substrate and Sn solder. Therefore, the thickness of the IMC layer must be controlled to ensure a better solder joint in the electronic packaging industry.

(Received December 19, 2018; accepted June 26, 2019; published online July 8, 2019)

Recently, ultrasonic-assisted brazing, a well-known fluxless brazing method, has been widely studied for soldering in the electronics industry owing to its excellent properties.[6–8] Previous studies have shown that the propagation of ultrasonic waves in a liquid solder can generate acoustic cavitation and streaming phenomena at the interface, which not only breaks the oxide film on the solid surface, but also improves the wetting of the liquid metal on the solid surface and promotes the diffusion of atoms.[9,10] Xiao et al.[11] brazed a Cu/Al substrate with Zn-3Al as a brazing filler metal, showing that excellent metallurgic bonding could be obtained in fluxless brazed Cu/Al joints by using ultrasonic-assisted soldering (UAS). Li et al.[12] also found that soldering time could be greatly shortened—and an excellent joint could be obtained—at lower soldering temperatures in the ultrasonic-assisted transient liquid phase (TLP) soldering process, which helped avoid extra thermal stress from excessive temperature or longer soldering times on the bond components. All these studies

indicated that UAS has become the most promising soldering technology for application to electronic component packaging. However, there is little research on the formation and evolution of IMCs or their effects on joint properties when using UAS. Therefore, this study employs the Cu-Sn system to study the formation and evolution of IMCs by UAS. Its results can provide theoretical guidance for the application of UAS in microelectronic packaging.

EXPERIMENTAL PROCEDURES

Highly pure (99.99 wt.%) 50 mm × 20 mm × 3 mm and 40 mm × 20 mm × 3 mm Cu plates were used as substrates, and pure (99.99 wt.%) 10 mm × 15 mm × 0.3 mm Sn plates were used as the solder. Before performing the brazing experiment, the Sn foils were cleaned with a detergent solution, then rinsed with deionised water, and finally cleaned using acetone in an ultrasonic bath for 3 min. The surfaces of Cu substrates were first ground and polished. Then they were cleaned using 5% HCl in an ultrasonic bath for 3 min and finally cleaned using acetone, also in an ultrasonic bath for 3 min. Figure 1 shows a schematic of UAS.

The Cu/Sn/Cu structure was placed in a furnace and heated at a rate of 50°C/min up to 300°C and then held for 6 min at 300°C during the process of soldering. The horizontal ultrasonic vibration frequency was fixed at 20 kHz, a pressure of 0.6 MPa, and power of 500 W. After applying ultrasonic waves, samples were derived from the heating platform and quickly cooled in water. The mounted samples were successively ground using #800, #1000, #1500, #2000, and #3000 metallographic sandpaper. Finally, the samples were polished mechanically using 0.5 μm diamond polishing paste. Subsequently, a few samples were deeply etched in a 5% HCl + 3% HNO_3 + CH_3OH (wt.%) etchant solution to remove the excess Sn solder so that the formation of interfacial Cu_6Sn_5 grains can be investigated during soldering. The microstructures of the joints were examined using backscattered electron signals from an EDS-equipped FEG 450 scanning electron microscope (SEM), including the distribution of Cu and Sn atoms, and the formation and evolution of Cu-Sn IMCs by UAS. In addition, the average thickness of the IMC layer in these samples was also determined by counting the total area and length of the IMCs along the interface in the SEM images, and it was calculated using the following equation[13]:

$$H = \frac{S}{L} \tag{1}$$

where H is the average thickness of the IMCs, S is the total IMC area (including Cu_6Sn_5 and Cu_3Sn), and L is the total length of the interface in the SEM images for one sample.

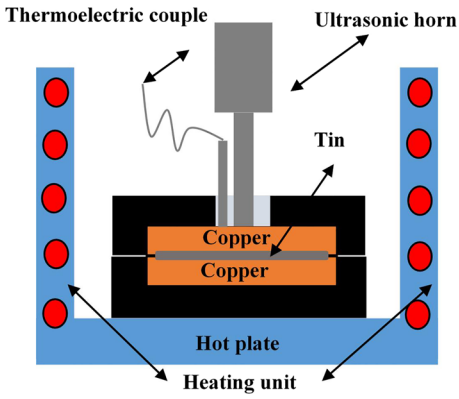

Fig. 1. Schematic of ultrasonic-assisted soldering.

RESULTS AND DISCUSSION

The Relationship Between IMC Thickness and Ultrasonic Action Time

Figure 2 shows the microstructures of the Cu-Sn joints formed via UAS at 300°C for various ultrasonic action times. Figure 2a shows a morphology photograph of joints soldered for 6 min without ultrasonic action, where the IMC layer is scallop-shaped. As presented in Table I, an EDS analysis revealed that the reaction layer labelled as '1' is Cu_6Sn_5. The dark, thin layer labelled as '2' is a layer of Cu_3Sn, which is consistent with previous literature.[14,15] A few Cu_6Sn_5 particles labelled as '3' are randomly distributed in the Sn solder. Figure 2b shows a photograph of the morphology of joints after ultrasonic action for 10 s, in which the morphology of the interfacial IMC layers has changed slightly. However, the volume of Cu_6Sn_5 in the Sn solder has significantly increased. Figure 2c and d show the microstructure of joints with ultrasonic action time of 20 s and 30 s, respectively. Note that the volume of Cu_6Sn_5 in the Sn solder further increased, and the Cu_6Sn_5 layer was crushed after ultrasonic action for 30 s. When the ultrasonic action time was increased to 40 s, the interfacial IMC layer was clearly crushed, as shown in Fig. 2e, the scallop-shaped compound layer disappeared, and the Cu_3Sn layer was also crushed. Simultaneously, the morphology of the compound in the Sn solder transformed from a strip block to a multi-planar layer.[16] This change in IMC morphology was more evident when ultrasonic vibration was applied for 50 s, as shown in Fig. 2f.

Figure 3 demonstrates SEM images of Cu-Sn samples after ultrasonic action for 50 s, in which three broken pits can be observed in the IMC layer. Further analysis revealed that the broken pits labelled as '1' are only Cu_6Sn_5. The broken pits labelled as '1' are Cu_3Sn, Cu_6Sn_5, and the Cu substrate, and some Cu_3Sn could also be found in broken pits '3'.

Figure 4 demonstrates the relationship between the thickness of the IMC layer and ultrasonic action

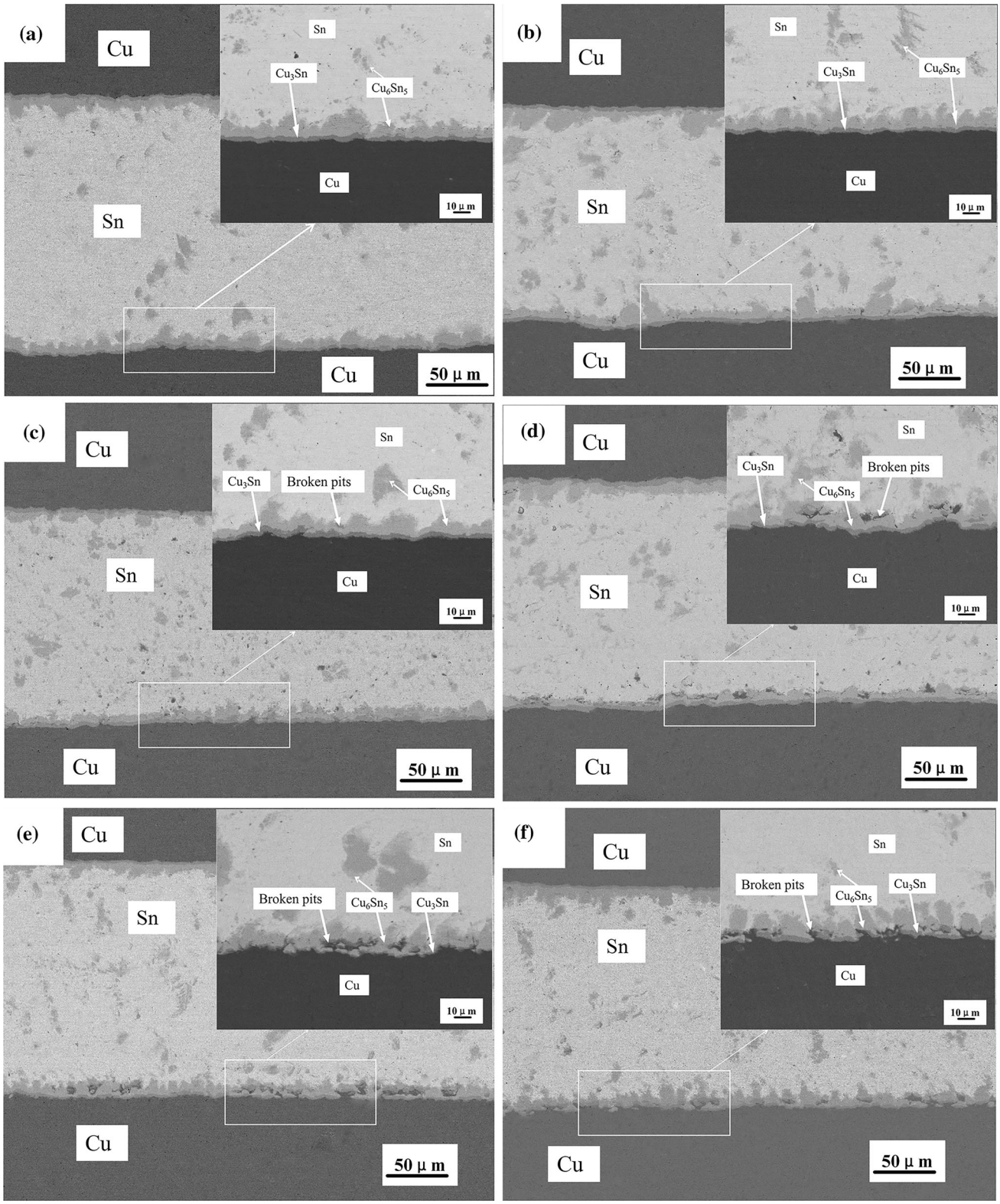

Fig. 2. SEM images of Cu-Sn samples after ultrasonic action for (a) 0 s, (b) 10 s, (c) 20 s, (d) 30 s, (e) 40 s, and (f) 50 s.

time, and the thickness of the total IMC layer and that of the Cu_6Sn_5 layer decreased with increasing ultrasonic action time. However, the Cu_3Sn layer initially increased with ultrasonic action for around 30 s, then decreased after the ultrasonic bonding time increased to 40 s.

Figure 5 shows the relationship between the IMC in the Sn solder and ultrasonic action time. The distribution area of the Cu_6Sn_5 in the Sn solder was increased with the propagation of ultrasonic waves. Additionally, the interfacial IMC layer was also thinned with increasing ultrasonic action time. Therefore, it could be inferred that the interfacial IMCs were crushed, and their formation was promoted by ultrasonic action.

Table I. Chemical composition at different locations in Cu-Sn joints in Fig. 2 (at.%)

Location	Cu (at.%)	Sn (at.%)
1	55.6	44.4
2	72.8	27.2
3	50.2	49.8

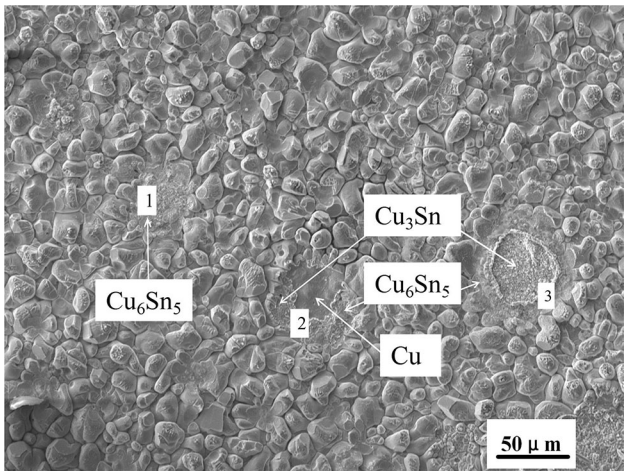

Fig. 3. SEM images of Cu-Sn samples after ultrasonic action for 50 s.

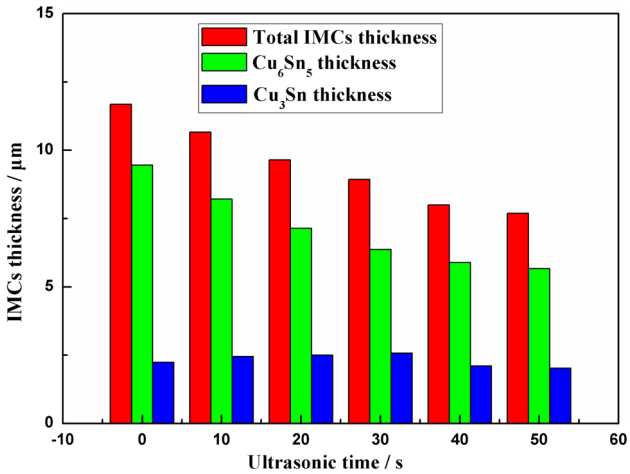

Fig. 4. Relationship between the thickness of the IMC layer and ultrasonic action time in Cu-Sn samples.

The translation of Cu_6Sn_5 in Sn solder is given in the following equation:

$$Y = AX^2 + BX + C \tag{2}$$

where Y is the area of Cu_6Sn_5 in the Sn solder, and X is ultrasonic action time. The values of A, B, and C were found from the fitting to be as -0.26916 ($\pm$ 0.07908), 36.75435 ($\pm$ 4.25974), and 2140.50186 ($\pm$ 44.32127), respectively.

If the shape of Cu_6Sn_5 in Sn solder is considered to be a circle, where the radius, i.e. the equivalent circular radius, can be obtained by Eq. 3, R is the equivalent circular radius of the Cu_6Sn_5 in the Sn solder. According to this analysis, Z is linear with X, as shown in Fig. 5b. That is, the formation of Cu_6Sn_5 in the Sn solder was mainly controlled by the reaction in Eq. 4.[17]

$$R = \sqrt{\frac{Y}{\pi}} \tag{3}$$

$$R = DX + E \tag{4}$$

where X is the ultrasonic action time, and D and E were found from the fitting to be 0.11189 ($\pm$ 0.00851) and = 27.11665 ($\pm$ 0.28593), respectively.

The above analysis found that the application of ultrasonic waves not only promotes the diffusion of Cu atoms, but also accelerates the growth of compounds in the Sn solder. Previous studies have shown that propagation of ultrasonic waves in a liquid medium can generate acoustic cavitation phenomena,[18] in which numerous micro-bubbles are generated and grow significantly. When these bubbles approach the solid–liquid interface, they rapidly implode because their movement is hampered, which can induce a localised high-temperature, high-pressure environment and micro-jet phenomena at the Cu/Sn solid–liquid interface.[19] Simultaneously, the exploding bubbles can form a powerful shock wave,[20] which accelerates the turbulent flow of the liquid. The high-speed fluid would constantly flush the surface of the base metal and the previously formed IMC layer. As shown in Fig. 2c and d, the pre-formed IMC layer at the interface was constantly crushed by the shock waves and cavitation bubbles, which led the scallop-like IMC layer to disappear and a few crushed pits to form at the Cu/Sn solid–liquid interface. For ultrasonic action time up to 40 s, the broken pits appeared in the Sn/Cu_6Sn_5 and Cu_3Sn/Cu_6Sn_5 interfaces, as shown in Fig. 2e. The same phenomenon could be observed after ultrasonic action for 50 s, as shown in Fig. 2f. In addition, the pre-formed IMC layer in the solid–liquid interface could obstruct the diffusion of Cu atoms into the Sn solder at ultrasonic action times of around 30 s, which causes a few of the Cu atoms to diffuse from the base

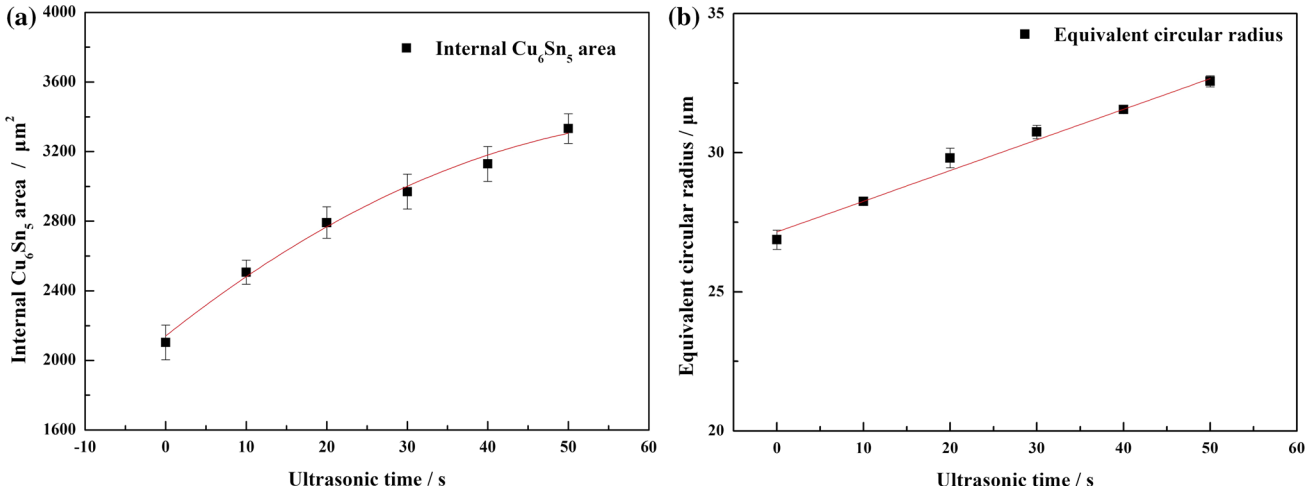

Fig. 5. (a) Area of Cu_6Sn_5 in the Sn solder and (b) An equivalent circular radius of Cu_6Sn_5 in Sn solder as functions of the ultrasonic action time.

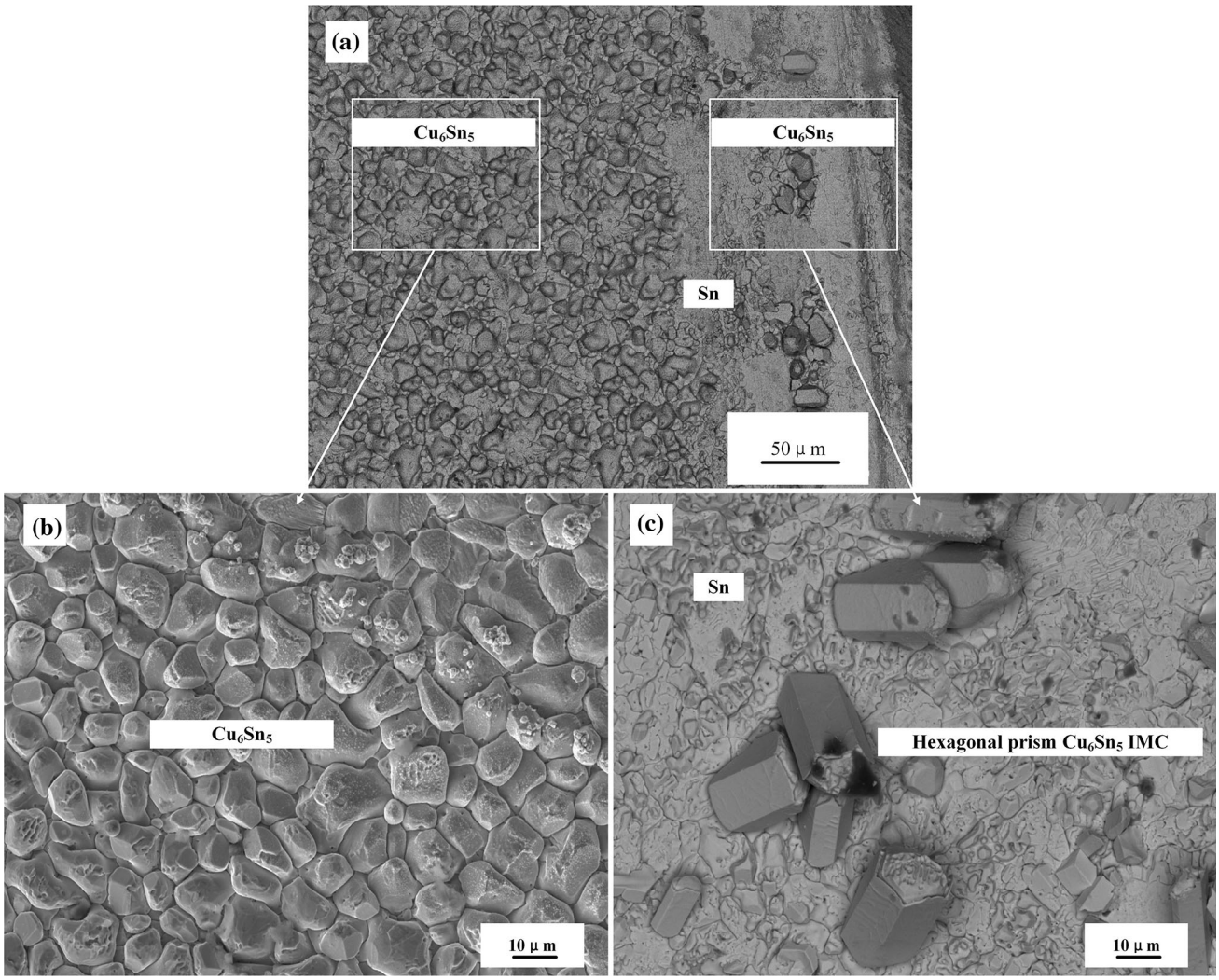

Fig. 6. Morphology of Cu-Sn samples with IMCs in the joint (a), at the interface (b), and in the Sn solder (c) after bonding for 6 min at 300°C.

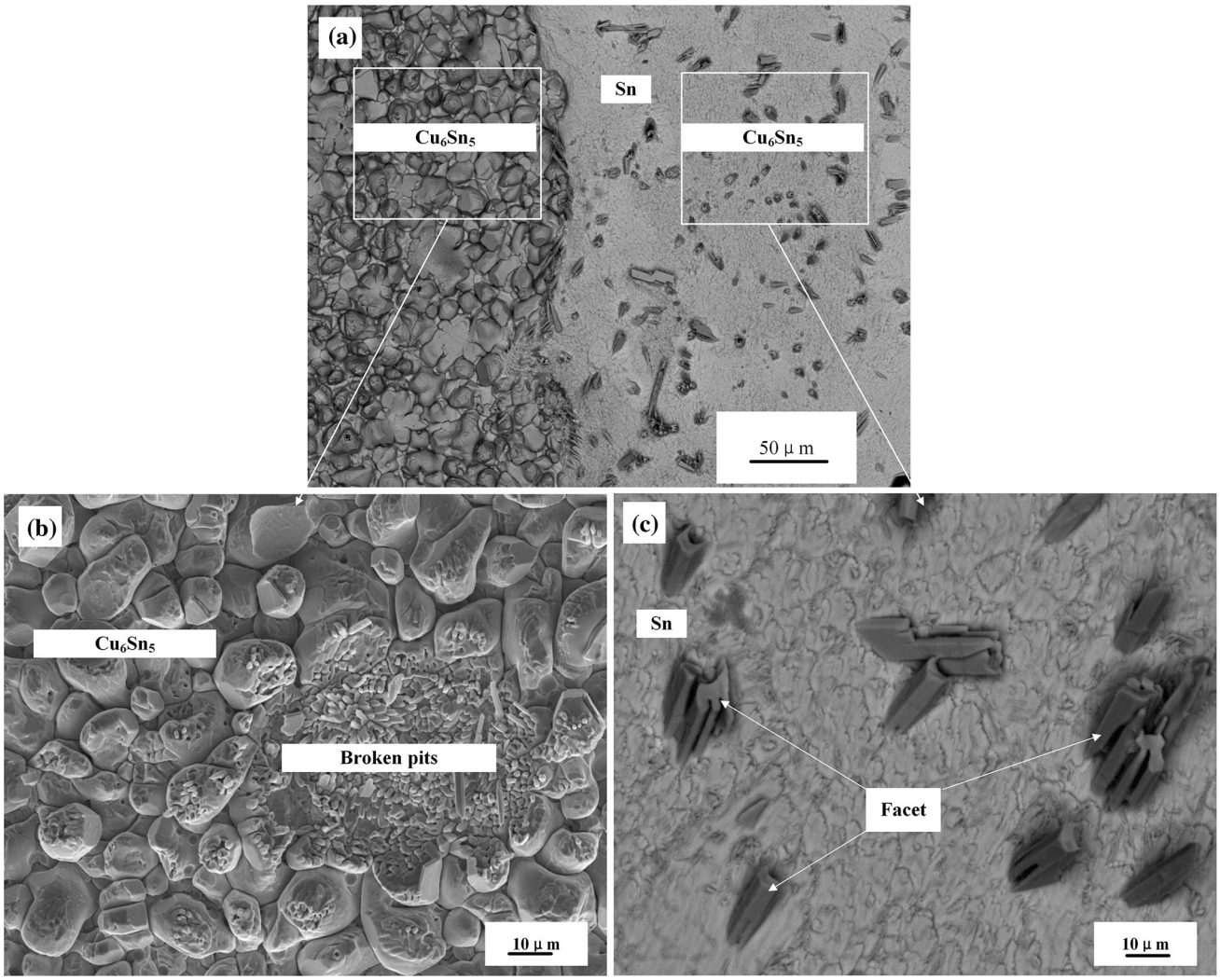

Fig. 7. Morphology of Cu-Sn IMCs in the joint (a), at the interface (b), and in the Sn solder (c) after ultrasonic action for 40 s.

metal to accumulate at the Cu_3Sn/Cu_6Sn_5 interface. Meanwhile, shock waves, cavitation bubbles, and localised high temperatures led to micro-damages of the solid Cu surface, which produced an excessive number of Cu atoms detached from the Cu surface and spread into the molten Sn solder. The additional Cu atoms provide excellent conditions for the formation of Cu_3Sn. Note that the average thickness of the Cu_3Sn layer slowly increased during ultrasonic action times in the range of 30 s, as shown in Fig. 4. However, when the ultrasonic action time increased to 40 s, the average thickness of the Cu_3Sn layer began to decrease, which was attributed to the crushing of the IMC layer. The crushed IMC layer could provide a few new diffusion channels for Cu and Sn atoms, which makes it easier for the Cu atoms to dissolve away from the base metal to diffuse into the Sn solder under the effect of chemical gradients and acoustic flow. Cu_6Sn_5 generated in the Sn solder with ultrasonic action times of 40 s and 50 s, shown in Fig. 2e and f, differed from its generation in the Sn solder with ultrasonic action times of approximately 30 s.

Morphology of Interfacial IMCs by UAS

As shown in Figs. 6 and 7, the joints were pulled away in two parts from the bonding surface, one of which was ground layer by layer until the IMC layer was observed by SEM. Figure 6 shows the grain morphology of Cu_6Sn_5 without ultrasonic action. The Cu_6Sn_5 grains at the Sn/Cu interface were mainly scallop-shaped, as shown in Fig. 6b, whereas the Cu_6Sn_5 grains generated in the Sn solder were regular hexagonal prisms, as shown in Fig. 6c. Figure 7 illustrates the grain morphology of Cu_6Sn_5 with ultrasonic action for 40 s. Although the grain morphology of Cu_6Sn_5 at the Sn/Cu interface was still scallop-like in shape, a few obviously broken pits in the interfacial Cu_6Sn_5 layer could be found.

Simultaneously, the grain morphology of Cu_6Sn_5 in the Sn solder was in the facet-shaped instead of a regular hexagonal prism, meaning that the ultrasonic action could cause the interfacial IMC layer to be crushed and the growth pattern of Cu_6Sn_5 grains in the Sn solder to be transformed.

According to Jackson,[21] atomic geometry—including facet- or round-shaped geometry—is mainly determined by the Jackson's coefficient of the crystal. Choi et al.[22] extended Jackson's theory to the grain morphology of the IMC that forms at the interface between liquid solder and solid–metal substrates. The morphology of IMCs was also found to be related to Jackson's coefficient. That is, Jackson's coefficient of a round grain is always less than 2, but Jackson's coefficient for a faceted grain is greater than 2. Jackson's coefficient depends largely on enthalpy changes, its value is modified as follows:

$$\alpha = \frac{\Delta H}{RT}\xi \tag{5}$$

where α is Jackson's coefficient, ΔH is the enthalpy change during the reaction of the liquid solder and the metal substrate into an IMC, R is a gas constant, T is the soldering temperature, and ζ is an atomic fraction of possible sites occupied by solid atoms at the growing interface. Because it is difficult to calculate the exact value of ζ—owing to the random orientation between adjacent IMC grains—a mean value of $\zeta = 0.5$ can be found in close-packed planes (0001) of hexagonal Cu_6Sn_5 was used to find out the different growth patterns of Cu_6Sn_5 grains. According to Kirchhoff's law, enthalpy changes are related to the reaction temperature using the following equation:

$$\Delta H = A_0 + A_1 T + A_2 T^2 \tag{6}$$

Yang et al.[23] showed that the values of A, A_0, and A_1 in a pure Sn/Cu system are 19064.81, − 75.08, and 0.11 respectively. Thus, a value of $\alpha = 1.28$ can be calculated by Eq. 5 at 300°C. This value is less than 2, showing that round Cu_6Sn_5 grains grow while holding at 300°C, which is consistent with the behaviour seen in the experiment shown in Fig. 6a. Meanwhile, Cu_6Sn_5 formed in the Sn solder when a few of the Cu atoms diffused into liquid Sn. Since the Cu_6Sn_5 grains had a close-packed hexagonal structure, they grew in hexagonal prisms along the screw dislocations by means of a step mechanism and extended into the Sn solder, as shown in Fig. 6c. However, when ultrasonic vibration was applied, the cavitation bubbles rapidly collapsed, which creates hot spots with the localised temperature and pressure estimated to reach 5000 K and 0.1 GPa, respectively. The liquid near the cavitation bubble is also affected, and its effective temperature can reach 1600°C.[24] The enthalpy change in the entire joint increased owing to the high-temperature, high-pressure environment. Substituting the effective temperature into Eq. 5, Jackson's coefficient was calculated as 8.49—considerably greater than 2—meaning that the Cu_6Sn_5 grains grow in a facet-shaped geometry under ultrasonic action. Furthermore, Cu and Sn atoms continuously underwent interdiffusion, driven by the temperature and concentration gradients before applying ultrasonic action, but the speed of diffusion was relatively slow. Thus, the Cu atoms that diffused into Sn solder gathered at the Cu/Sn solid–liquid interface. However, when ultrasonic waves were applied, the action of ultrasonic waves caused the liquid Sn to continuously flow at a high speed. This instantaneously brought the Cu and Sn atoms into the liquid Sn under the action of the acoustic current, resulting in a new concentration gradient at the Cu/Sn solid–liquid interface, which accelerated the dissolution rate of base metals into the liquid solder. The effect of the ultrasonic waves made it difficult for Cu atoms to gather inside the Sn solder. To reduce the nucleation energy, precipitation usually took place at the existing IMC interface, as the liquid solder would otherwise be supersaturated. Therefore, the growth of Cu_6Sn_5 grains was considerably enhanced, and the dissolution of Cu atoms was considerably improved, leading to a facet-shaped geometry, as shown in Fig. 7.

In addition, the application of ultrasonic waves can induce intense acoustic streaming in liquids, which accelerate the dissolution rate of base metals into the liquid solder by promoting elemental diffusion in the liquid solder at high speed. Therefore, the Sn solder was in a dynamic non-equilibrium state such that IMCs at the Cu/Sn solid–liquid interface were crushed continuously, dissolved, and formed by UAS. Some crushed Cu_6Sn_5 enters the Sn solder, and others dissolve at the local high temperatures. The dissolved Cu and Sn atoms provided conditions for the growth of Cu_6Sn_5. Meanwhile, ultrasonic vibration and agitation relied on external input energy, promoted the formation of internal Cu_6Sn_5 crystal nuclei, and fractured the growing dendrites. More Cu_6Sn_5 grains formed and were evenly distributed in the joint after cooling, which would improve the performance of welded joints.[25,26]

CONCLUSIONS

The effects of UAS on the microstructure of Cu-Sn IMCs were investigated, and the major conclusions can be summarised as follows:

1. When ultrasonic waves were introduced to the soldering joint, the IMC dendrites generated at the Cu/Sn solid–liquid interface broke, which led to a severe decrease in the thickness of the Cu_6Sn_5 and Cu_3Sn layers.
2. The ultrasonic vibration and agitation promoted the nucleation of Cu_6Sn_5 crystals in the Sn solder, which was kept in a dynamic non-equilibrium state with IMCs at the Sn/Cu interface and in the Sn solder.

3. With the propagation of ultrasonic waves, the enthalpy of the Cu-Sn system increased, and Cu_6Sn_5 grains in the Sn solder grew into facet shapes instead of round shapes.

ACKNOWLEDGMENTS

This work was supported financially by the National Natural Science Foundation of China (Nos. 51465032 and 51665031).

REFERENCES

1. X. Ma, Y. Qian, and F. Yoshida, *J. Alloys Compd.* 334, 224 (2002).
2. Y. Zhou, F. Liu, and H. Wang, *Polym. Compos.* 38, 803 (2017).
3. C. Hang, Y. Tian, R. Zhang, and D. Yang, *J. Mater. Sci. Mater. Electron.* 24, 3905 (2013).
4. N.S. Bosco and F.W. Zok, *Acta Mater.* 52, 2965 (2004).
5. T. Laurila, V. Vuorinen, and M. Paulasto-Kröckel, *Mater. Sci. Eng. R Rep.* 68, 1 (2010).
6. T.H. Kim, J. Yum, S.J. Hu, J.P. Spicer, and J.A. Abell, *CIRP Ann.* 60, 17 (2011).
7. A. Panteli, J.D. Robson, I. Brough, and P.B. Prangnell, *Mater. Sci. Eng. A* 556, 31 (2012).
8. W. Guo, T. Luan, X. Leng, J. He, and J. Yan, *Trans. Nonferrous Met. Soc. China* 27, 962 (2017).
9. K.M. Hafez, M.H. El-Sayed, and M. Naka, *Sci. Technol. Weld. Joining* 10, 125 (2013).
10. W. Cui, C. Wang, J. Yan, Z. Wang, and D. Wei, *Ultrason. Sonochem.* 20, 196 (2013).
11. Y. Xiao, H. Ji, M. Li, and J. Kim, *Mater. Des.* 52, 740 (2013).
12. M. Li, Z. Li, Y. Xiao, and C. Wang, *Appl. Phys. Lett.* 102, 094104 (2013).
13. B.-H. Kwak, M.-H. Jeong, J.-W. Kim, B. Lee, H.-J. Lee, and Y.-B. Park, *Microelectron. Eng.* 89, 65 (2012).
14. J.F. Li, P.A. Agyakwa, and C.M. Johnson, *Acta Mater.* 59, 1198 (2011).
15. H. Liu, K. Wang, K.E. Aasmundtveit, and N. Hoivik, *J. Electron. Mater.* 41, 2453 (2012).
16. M.S. Park, S.L. Gibbons, and R. Arróyave, *Microelectron. Reliab.* 54, 1401 (2014).
17. B.-J. Kim, G.-T. Lim, J. Kim, K. Lee, Y.-B. Park, H.-Y. Lee, and Y.-C. Joo, *J. Electron. Mater.* 39, 2281 (2010).
18. K.S. Suslick, *Sci. Am.* 260, 80 (1989).
19. S.D. Hyman, T.J. Lazio, N.E. Kassim, P.S. Ray, C.B. Markwardt, and F. Yusef-Zadeh, *Nature* 434, 50 (2005).
20. E.A. Brujan, T. Ikeda, and Y. Matsumoto, *Exp. Therm. Fluid Sci.* 32, 1188 (2008).
21. K.A. Jackson, *Prog. Solid State Chem.* 4, 53 (1967).
22. W.K. Choi, S.-Y. Jang, J.H. Kim, K.-W. Paik, and H.M. Lee, *J. Mater. Res.* 17, 597 (2011).
23. M. Yang, M. Li, and C. Wang, *Intermetallics* 25, 86 (2012).
24. K.S. Suslick, D.A. Hammerton, and R.E. Cline, J. Am. Chem. Soc. 89 (1986).
25. X. Leng, C. Wang, Y. Zhang, X. Chen, and J. Yan, *Trans. Nonferrous Met. Soc. China* 21, s290 (2011).
26. T. Luan, W. Guo, S. Yang, Z. Ma, J. He, and J. Yan, *J. Mater. Process. Technol.* 248, 123 (2017).